Novel bisretinoids of human retina are lyso alkyl ether glycerophosphoethanolamine-bearing A2PE species[S]

Hye Jin Kim* and **Janet R. Sparrow**[1],*,[†]

Departments of Ophthalmology* and Pathology and Cell Biology,[†] Columbia University Medical Center, New York, NY 10032

Abstract Bisretinoids are a family of fluorophores that form in photoreceptor cells' outer segments by nonenzymatic reaction of two vitamin A aldehydes (A2) with phosphatidylethanolamine (PE). Bisretinoid fluorophores are the major constituents of the lipofuscin of retinal pigment epithelium (RPE) that accumulate with age and contribute to some retinal diseases. Here, we report the identification of a previously unknown fluorescent bisretinoid. By ultraperformance LC (UPLC) coupled to photodiode array detection, fluorescence (FLR), and ESI-MS, we determined that this novel bisretinoid is 1-octadecyl-2-lyso-*sn*-glycero A2PE (alkyl ether lysoA2PE). This structural assignment was based on molecular mass (m/z 998), UV-visible absorbance maxima (340 and 440 nm), and retention time (73 min) and was corroborated by biomimetic synthesis using all-*trans*-retinal and glycerophosphoethanolamine analogs as starting materials. UPLC profiles of ocular extracts acquired from human donor eyes revealed that alkyl ether lysoA2PE was detectable in RPE, but not neural retina. LysoA2PE FLR spectra exhibited a significant hyperchromic shift in hydrophobic environments. The propensity for lysoA2PE to undergo photooxidation/degradation was less pronounced than A2E. In mechanistic studies, A2PE was hydrolyzed by phospholipase A_2 and plasmalogen lysoA2PE was cleaved under acidic conditions.[JLR] The characterization of these additional members of the bisretinoid family advances our understanding of the mechanisms underlying bisretinoid biogenesis.—Kim, H. J., and J. R. Sparrow. **Novel bisretinoids of human retina are lyso alkyl ether glycerophosphoethanolamine-bearing A2PE species.** *J. Lipid Res.* 2018. 59: 1620–1629.

Glycerophospholipids (GPs) are subdivided into distinct classes based on the nature of the polar head group at the *sn*-3 position of the glycerol backbone; the head group can be either choline or ethanolamine and, to a lesser extent, inositol or serine (1, 2). The *sn*-1 or *sn*-2 positions in the GP species are typically occupied by fatty acids (diacyl) linked to the glycerol backbone by ester bonds. Hydrolysis at either the *sn*-1 or *sn*-2 fatty acyl ester bond of phosphoglycerides produces free fatty acids and lysophospholipids (3). Diversity is also introduced to this structure by having a single alkyl chain at the *sn*-1 position linked to the glycerol via an ether bond (**Fig. 1**).

Ether GP species differ from the more common diacyl subclass in having a straight chain fatty alcohol rather than a fatty acid at the *sn*-1 position (2). The fatty alcohols are mainly restricted to saturated C16 (C16:0) or saturated and mono-unsaturated C18 (C18:0, C18:1) (2). Among these, ether-bonded GPs, those bearing vinyl ether (-O-C=C-) at the *sn*-1 position, are called plasmalogens (supplemental Fig. S1) (4). At the *sn*-2 position, plasmalogens are enriched in long-chain polyunsaturated fatty acids, specifically DHA (C22:6, ω-3) or arachidonic acid (C20:4, ω-6) (2). DHA is more abundant in the outer segments of photoreceptor cells than in any other mammalian cell membrane; 22:6*n*-3 accounts for 34.2% of the fatty acid in phosphatidylethanolamine (PE), 19.5% of the fatty acid in phosphatidylcholine (PC), and 34.1% of the fatty acid in phosphatidylserine (5).
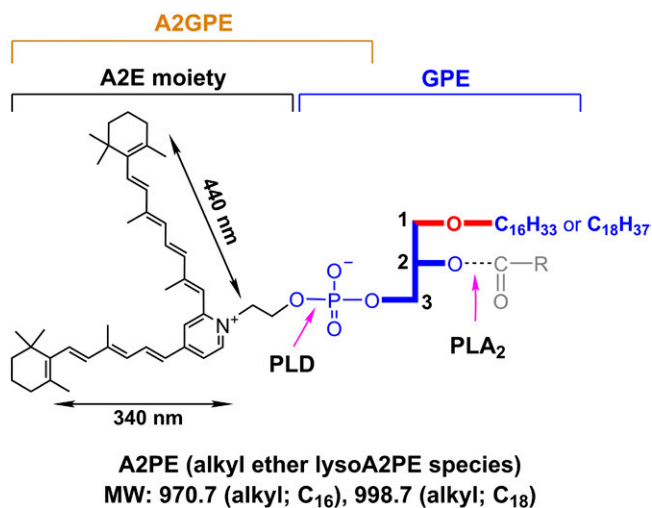
Fig. 1. Molecular weight (MW) and UV-visible absorbance (nm) of alkyl ether lysoA2PE. The structure includes an ether-linked (-O-) saturated alkyl chain, either C_{16} or C_{18} at the *sn*-1 position. Positions on the GPE that are subject to hydrolysis by PLA_2 and PLD are indicated (pink arrows). Cleavage by PLA_2 yields lysoA2PE. Cleavage by PLD yields A2E. Carbon numbers on the glycerol backbone are indicated by 1, 2, and 3. Absorbance peaks at 440 and 340 nm can be assigned to the long and short arms of the molecule, respectively.

The primary amine of PE in photoreceptor cell outer segments is notable for being subject to the reactivity of vitamin A aldehyde (all-*trans*-retinal or 11-*cis*-retinal) (6) that is essential to photon absorption by photoreceptor cells. The resulting Schiff base adduct, *N*-retinylidene-PE (NRPE) (7), serves to chaperone reactive retinaldehyde until it is reduced to all-*trans*-retinol by NADPH-dependent retinol dehydrogenases (RDHs) (RDH8, RDH11, and RDH12) in the cytoplasm of photoreceptor cells. A portion of NRPE is aided in its delivery to RDH by the photoreceptor-specific ABCA4 in outer segments (8–11).

Under some conditions, not all of which have been clarified, NRPE, instead of hydrolyzing to release PE, reacts nonenzymatically with a second molecule of retinaldehyde. The first step in this condensation reaction is a [1,6]-proton tautomerization generating a PE-retinyl enamine, which reacts with the second retinaldehyde. After aza-6π-electrocyclization and auto-oxidation of the dihydropyridinium intermediate (dihydro-A2PE) (12), the fluorescent phosphatidyl-pyridinium bisretinoid, A2PE, is formed. A2PE is not a single compound; rather, it consists of a mixture of retinaldehyde adducts having fatty acids of varying lengths and numbers of double bonds, stearic acid (18:0) and DHA (22:6) being two of these (13). These A2PE compounds are the immediate precursors of A2E, a prominent and well-known pigment of retinal pigment epithelium (RPE) lipofuscin. A2E is generated from A2PE by phosphate hydrolysis and this cleavage can be mediated by phospholipase D (PLD): incubation of A2PE in the presence of PLD results in the appearance of A2E in chromatographic profiles (14). Hydrolytic activity in lysosomes isolated from liver and RPE also release A2E from A2PE (15). Additionally, this activity can be inhibited by the PLD inhibitor, calphostin C, and by a protease inhibitor cocktail.

After phosphate cleavage of A2PE, no further degradation of the molecule occurs.

Reactions of retinaldehyde with PE lead to the formation of not only A2PE but also other fluorophores that constitute a complex mixture of fluorescent bisretinoid compounds within the lipid bilayer of the photoreceptor outer segment. These other bisretinoid fluorophores include the phosphatidyl-dihydropyridine bisretinoid, A2-dihydropyridine-PE (A2-DHP-PE), and both the all-*trans*-retinal dimer and the related PE conjugate, all-*trans*-retinal dimer-PE (14, 16–19). The nomenclatures assigned to these compounds were designed to indicate both the structures and the formation from two retinaldehyde (vitamin A-aldehydes; A2) molecules. The structures of these bisretinoids have been demonstrated by MS and NMR spectroscopy together with biomimetic synthesis, and all of these compounds present with a head group from which two polyene hydrophobic arms extend, each serving as a chromophore exhibiting absorbance in the visible or UV range. Due to the continual turnover of outer segment membrane combined with phagocytic clearance by adjacent RPE cells (20), these bisretinoid pigments do not accumulate in photoreceptor cells but, instead, are transferred to the RPE and become the lipofuscin of these cells. While these fluorophores accumulate even in healthy eyes, deficiency in ABCA4 due to gene mutation in humans and mice leads to elevated levels of both *N*-retinylidene-PE and the various bisretinoids (17, 21–23).

Because A2E is a substantial peak in RPE extracts and A2PE is present at relatively low or nondetectable levels, hydrolytic cleavage of A2PE with release of A2E and, presumably, phosphatic acid appears to occur as a facile reaction. Conversely, the relative abundance of A2-DHP-PE (19) and all-*trans*-retinal dimer-PE (17) in mouse eyecups and human and bovine RPE, indicates that these bisretinoids are relatively refractory to cleavage. The same can be said for A2-glycerophosphoethanolamine (A2GPE), an ethanolamine ester of glycerophosphoric acid. ^{1}H-NMR and ^{13}C-NMR spectra of A2GPE confirmed the presence of the glycerol and phosphate moieties (24).

Our chromatographic and spectroscopic analyses of the fluorophores in human retina have revealed compounds that we have not previously identified. Notably, the fluorescent molecules that attract attention exhibit absorbances in both the UV and visible range. This is a signature feature of bisretinoids. Here, we report the structures, mechanisms of formation, and photooxidative properties of two newly recognized fluorophores.

MATERIALS AND METHODS

Animals and tissues

Purified bovine rod outer segments (ROSs) were purchased from InVision BioResources (Seattle, WA). Human donor eyes (age range 26–74 years, six eyes) were received within 24 h of death from the Eye-Bank for Sight Restoration (New York, NY). The study was in accordance with the Declaration of Helsinki with regard to the use of human tissue. Bovine ROSs and human RPE/choroid and neural retina were homogenized in DPBS using a

tissue grinder in the presence of chloroform/methanol (1:1). Subsequently, the sample was extracted three times with addition of chloroform and centrifuged at 3,220 g for 10 min. After passing through a filter, the extract was concentrated by evaporation of solvent under argon gas and redissolved in ethanol. The sample was centrifuged at 21,130 g for 3 min and the supernatant was transferred to the ultra-performance (UP)LC autosampler and the supernatant was analyzed by UPLC.

UPLC-MS

MS was performed on a Waters Acquity UPLC system (Waters, Milford, MA) that was coupled online with a single quadrupole mass spectrometer (Waters SQD) and both photodiode array (PDA; Waters) and fluorescence (FLR; Waters) detectors. The mass spectrometer was equipped with ESI and the single quadrupole analyzer was set to operate in either full scan mode (ranging from m/z 150 to 2,000) or to scan a single mass unit (selected ion monitoring). For elution, a phenyl column (Waters ACQUITY UPLC® BEH phenyl; 1.7 µm, 2.1 × 100 mm) was used with a mobile phase of acetonitrile/water (1:1) and isopropanol/acetonitrile (9:1), both with 0.1% formic acid (UPLC condition a: 0–50 min, 100–55% acetonitrile/water in isopropanol/acetonitrile; 50–110 min, 55–35% acetonitrile/water in isopropanol/acetonitrile; flow rate of 0.2 ml/min), and an injection volume of 10 µl. All bisretinods, including isoA2E, A2E, A2GPE, A2-DHP-PE, all-*trans*-retinal dimer (atRALdi)-PE, A2PE, and lysoA2PE, were quantified using UPLC chromatograms together with software (Waters Empower 3). Additionally, for analysis of synthetic chemicals, the same phenyl column was used with a mobile phase of water and acetonitrile/methanol (1:1), both with 0.1% formic acid (UPLC condition b: 0–1 min, 30% acetonitrile/methanol; 1–27 min, 98% acetonitrile/methanol and then the final condition was held for 3 min; flow rate of 0.5 ml/min and an injection volume of 5 µl).

Biomimetic synthesis

A2E, A2GPE, A2-DHP-PE, atRALdi-PE, and A2PE species were synthesized as previously described (16, 19, 24, 25). The lysoA2PE was synthesized by treating one equivalent of 1-*O*-octadecyl-2-hydroxy-*sn*-glycero-3-phosphoethanolamine (custom synthesis; Avanti Polar Lipids Inc., Alabaster, AL) with two equivalents of all-*trans*-retinal in 0.1% trimethylamine containing chloroform/methanol (2:1) solution at 37°C in the dark for 3 days. The reaction mixture was dried under argon gas and redissolved and diluted in ethanol for UPLC analysis (UPLC condition a) as described above.

Spectroscopy

FLR spectra of alkenyl ether lysoA2PE (**Table 1**, compound 6) in indicated solvents were recorded in either a SpectraMaxM5

reader (Molecular Devices Inc, Sunnyvale, CA) using a 384-well microplate (polystyrene, flat-bottom, well depth of 11.56 mm) or a Luminescene Spectrometer LS55 (PerkinElmer, Shelton, CT) using a quartz cuvette (10 mm path-length) (luminescence spectroscopy cells; PerkinElmer) as indicated. FLR was recorded at room temperature as relative FLR units from 500 to 800 nm in 1 or 10 nm steps and using a bandpass slit of 6 nm and an excitation of 440 nm.

Hydrolysis of bisretinoids with enzymatic and nonenzymatic incubation

To test PLD activity (300 units/ml PLD from *Streptomyces chromofuscus*; Enzo Life Sciences, Framingdale, NY), alkenyl ether lysoA2PE (Table 1, compound 6) in DMSO (15 µl) was added to 485 µl DPBS buffer (with $CaCl_2$ and $MgCl_2$; GIBCO-Invitrogen, Carlsbad, CA). To assay phospholipase A_2 (PLA_2) (300 units/ml PLA_2 from porcine pancreas; Sigma-Aldrich, St. Louis, MO), alkenyl ether acylA2PE (Table 1, compound 7) in DMSO (15 µl) was added to 485 µl borax buffer (with 10 mM $CaCl_2$, pH 9). The mixtures were incubated for 24 h at 37°C. For a nonenzymatic hydrolysis experiment, 1-(1Z-octadecenyl)-2-hydroxy-*sn*-glycero A2PE (Table 1, compound 6) was incubated in DPBS (containing 2% DMSO) at pH 5 for 48 h at 37°C. After incubation, mixtures were extracted with chloroform, dried under argon, and analyzed by UPLC-MS (UPLC condition b) as described above.

Photooxidation of lysoA2PE

A2E, acyl lysoA2PE (Table 1, compound 5), and alkenyl ether lysoA2PE (Table 1, compound 6) (200 µl, 100 µM in DPBS at pH 7; 2% DMSO) were irradiated (430 nm) for 0, 30, 60, and 120 s after which each sample was injected into the column (Waters BEH phenyl) for analysis by UPLC-MS (UPLC condition b) as described above.

RESULTS

Analysis of unknown bisretinoids in human RPE extract by UPLC-PDA-FLR-MS

We analyzed whole chloroform/methanol extracts of human RPE/choroid (age range 26 to 74 years, six samples) by reverse-phase UPLC-FLR-MS with PDA detection at 430 nm. Peaks in the UPLC profile had retention times (Rts) assignable to the previously identified RPE bisretinoids: A2E and isoA2E, A2GPE, A2-DHP-PE, and atRALdi-PE (13, 16, 23, 24) (**Fig. 2A**). In addition, two peaks (Rts: 68 and 73 mins) reflecting slightly less polar compounds were

TABLE 1. List of A2PE species studied

Compound Identification[a]	Systematic Name	Common Name[b]	Exact Mass (m/z)	Retention Time (min)[c]
Compound 1	1-Hexadecyl-2-lyso-*sn*-glycero A2PE	Alkyl ether lysoA2PE (O-16:0/0:0)	970.7	68[a]
Compound 2	1-Octadecyl-2-lyso-*sn*-glycero A2PE	Alkyl ether lysoA2PE (O-18:0/0:0)	998.7	73[a]
Compound 3	1,2-Dihexadecanoyl-*sn*-glycero A2PE	Diacyl A2PE,A2-DPPE(16:0/16:0)	1,222.9	93[a]
Compound 4	1-Octadecanoyl-2- (4Z,7Z,10Z,13Z,16Z, 19Z-docosahexaenoyl)-*sn*-glycero A2PE	Diacyl A2PE [18:0/22:6 (4Z,7Z,10Z,13Z,16Z,19Z)]	1,323.0	101[a]
Compound 5	1-Octadecanoyl-2-lyso-*sn*-glycero A2PE	Acyl lysoA2PE (18:0/0:0)	1,012.7	19[b]
Compound 6	1-(1Z-octadecenyl)-2-hydroxy-*sn*-glycero A2PE	Alkenyl ether lysoA2PE (P-18:0/0:0)	996.7	21[b]
Compound 7	1-(1Z-octadecenyl)-2-(9Z-octadecenoyl)-*sn*-glycero A2PE	Alkenyl ether acyl A2PE [P-18:0/18:1(9Z)]	1,261.1	26[b]

[a] Compound identification denotes systematic and common name for quick indication.
[b] According to the LIPID MAPS system. GP abbreviations refer to species with one or two side-chains where the structures of the side chains are indicated within parentheses in the "headgroup(*sn*-1/*sn*-2)" format. Acyl chains are assumed by default. The "O-" prefix indicates the presence of an alkyl ether substituent; the "P-" prefix is used for the 1Z-alkenyl ether (plasmalogen) substituent.
[c] Nonitalic lowercase letters in this column denote UPLC conditions a and b as in Materials and Methods.
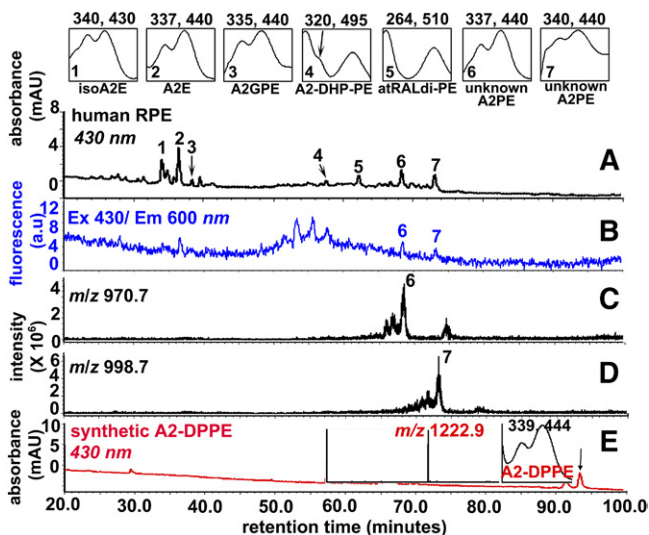
Fig. 2. UPLC profile of an extract of human RPE [donor age 74, 1 eye (A–D)]. A: Chromatogram with monitoring at 430 nm absorbance (UPLC condition a). Top insets: UV-visible absorbance spectra of isoA2E, A2E, A2GPE, A2-DHP-PE, atRALdi-PE, and unknown A2PE species. The chromatogram represents analysis of six eyes. B: FLR monitoring at an excitation of 430 nm and emission of 600 nm. C, D: Selected ion chromatogram at m/z 970.7 and 998.7 with Rts corresponding to peaks 6 and 7 in A. E: UPLC chromatogram (430 nm monitoring) detecting a synthetic product derived from a mixture of 1,2-dipalmitoyl-*sn*-glycero-3-phosphoethanolamine (DPPE) incubated with all-*trans*-retinal. Insets: Mass spectrum (left) and UV-visible absorbance spectrum (right) corresponding to indicated peak (A2-DPPE m/z 1,222.9) (arrow).

observed. The presence of two maxima in the absorbance spectra, one in the UV range and the other in the short-wavelength visible range, were suggestive of bisretinoid species (26) (Fig. 2A). Additionally, online FLR monitoring (excitation 430 nm/emission 600 nm) showed that the two unknown peaks of interest were fluorescent compounds (Fig. 2B). The m/z of these compounds were m/z 970.7 (Fig. 2C, peak 6) and 998.7 (Fig. 2D, peak 7). Due to the absorbance maxima and molecular mass, we considered the possibility that these peaks represented species of A2PE, the retinaldehyde-PE adducts, having variable fatty acid content, that serve as precursors of A2E. Based on the molecular mass and Rt, we excluded the A2PE species, A2-DPPE (Rt 93 min; m/z 1,222.9) (Table 1, compound 3), that is synthesized with DPPE (1,2-dipalmitoyl-*sn*-glycero-3-phosphoethanolamine) and all-*trans*-retinal as starting materials (Fig. 2E). From previous experience, we expected that detectable levels of A2PE would be quite low in human RPE extracts, a characteristic we have attributed to A2PE species being readily cleaved by PLD in RPE lysosomes (15). In bovine ROSs incubated with all-*trans*-retinal, A2-DPPE was not the major peak; instead the major A2PE species exhibited m/z 1,323.0 (supplemental Fig. S2).

UPLC profiles of tissue extracts from human neural retina and bovine ROSs

In samples of human neural retina and bovine ROSs, the peaks exhibiting m/z 970.7 and m/z 998.7 (peaks 6 and 7, respectively; Fig. 2C, D) were not detected (**Fig. 3**). Instead,
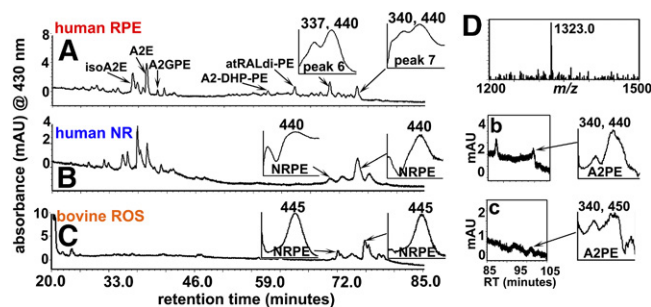

Fig. 3. UPLC chromatograms and monitoring at 430 nm (UPLC condition a). A: Human RPE. The UPLC injectant was hydrophobic extract of RPE/choroid (age 74 years, one eye). IsoA2E, A2E, A2GPE, A2-DHP-PE, atRALdi-PE, and two unknown peaks were detected. B: Human neural retina (NR) (35 years, one eye). C: Bovine ROSs (one eye). NRPE species: 440 nm; Rt 73–75 min (B, C). Peak 7 (Rt, 73 min in A). D: A2PE species detected in B and C exhibit m/z 1,323.0, consistent with stearic acid (C18:0) and DHA (C22:6) attached by ester linkages to GPE. b, c: Chromatogram (430 nm absorbance monitoring) expanded between Rts 85 and 105 min. A2PE peaks in the chromatogram and their corresponding UV absorbance spectra are shown.

as shown in Fig. 3, two peaks with similar Rts (Rts 68.5 and 73.2 mins) were observed. Due to their single maximum absorbance (λ_{max}) at 440 nm (Fig. 3B, C), we suspected that these peaks could be isomers of NRPE. On-line UPLC-MS indicated m/z values of 1,058 (Rt 73.2 mins) consistent with NRPE bearing stearic acid (C18:0) and DHA (C22:6 ω-3) at the *sn*-1 and -2 positions with the linkage to GPE being an ester (m/z values are not shown in Fig. 3) (13). This assignment was supported by the detection of diacyl A2PE (m/z 1,323.0, Rt 101 min) (Table 1, compound 4) attributable to GPE with stearic acid and DHA in hydrophobic extracts from human neural retina and bovine ROS (Fig. 3B, C). The presence of the latter diacyl A2PE species (13) was not surprising because DHA and stearic acid are abundant fatty acids from vertebrate ROS membrane (5).

Analysis of biosynthetic reaction mixtures

Ester-linked PEs and vinyl ether-linked PEs (the latter are commonly called plasmalogen) are the major sources of phospholipids in human outer segments of retina (27). Based on the molecular mass and Rts, we speculated that the two unknown peaks were A2PE species that bear a single saturated fatty acid chain (either C16:0 or C18:0) at the *sn*-1 position on glycerophosphoethanolamine (GPE) through an ether-linkage (Fig. 1). These ether-linked single alkyl chain A2PE species are here referred to as alkyl ether lysoA2PE (Table 1, compounds 1 and 2). In an attempt to identify peak 7 (m/z 998.7; Fig. 2) that was detected in human RPE, we incubated a custom-synthesized alkyl ether, lysoGPE(O-18:0/0:0), with all-*trans*-retinal at a 1:2 ratio. After incubation, the reaction mixture was analyzed by online UPLC-PDA-MS. The peak eluting from the synthetic mixture at 73.5 min presented with the same Rt (73.5 mins), UV-visible absorbance maxima (λ_{max} 340, 440 nm), and m/z 998.7 (peak 7, **Fig. 4**) as the peak that we detected in human RPE using the same analytic protocol (Fig. 2).
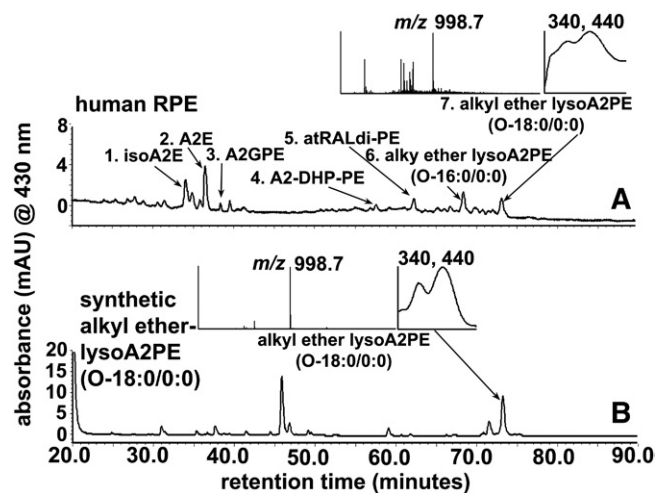
Fig. 4. Chromatographic separation by UPLC-ESI-MS with monitoring at 430 nm (UPLC condition a). A: Human RPE/choroid (same chromatogram as in Fig. 2A). B: A synthetic sample derived from the incubation of alkyl ether lysoGPE(O-18:0/0:0) with all-*trans*-retinal. Peak 7 corresponds to the equivalent peaks in A and Fig. 2A. Peak 7 in the human RPE sample elutes at the same Rt as the synthetic alkyl ether lysoA2PE(O-18:0/0:0) (m/z 998.7) in B. Insets top and bottom: UV-visible absorbance and mass spectra corresponding to indicated peaks (arrows)

A question that surrounded the ostensible ether-bearing lysoA2PE was whether the position of the single alkyl chain was either at *sn*-1 or *sn*-2 on the glycerol backbone of GPE. Thus, to clarify this issue, we used a series of analogs as starting materials in a synthetic mixture with 2 molecules of all-*trans*-retinal and analyzed a series of A2PE species by UPLC-PDA-MS.

Acyl lysoA2PE, which contains heptadecanoic acid (C17:0) attached at either the *sn*-1 or *sn*-2 through an ester linkage, was calculated to have an exact molecular mass of 998.70 corresponding to a chemical formula of $C_{62}H_{97}NO_7P^+$. Acyl lysoA2PE(17:0/0:0) eluted ∼2–3 min earlier and, furthermore, the other acyl lysoA2PE(0:0/17:0) eluted ∼3–4 min earlier than alkyl ether lysoA2PE (data not shown). Because an additional common source of GPE is alkenyl ether GPE (plasmalogen), we synthesized alkenyl ether lysoA2PE ($C_{63}H_{99}NO_6P^+$, m/z 996.7) (Table 1, compound 6) bearing the latter plasmalogen and analyzed by the same method. The chromatographic Rts of the alkenyl ether lysoA2PE(P-18:0/0:0) (supplemental Fig. S1; Table 1, compound 6) and alkyl ether lysoA2PE(O-18:0/0:0) (Fig. 1; Table 1, compound 2) were identical at ∼73.4 min, but the alkyl ether lysoA2PE could be easily distinguished by a 2 Da difference when the corresponding mass spectra were compared. Using our UPLC elution protocol (UPLC condition a), we were able to discriminate between the positions of single fatty acid chains based on Rt. From the comparison of biosynthetic experiments, the new A2PE constituents corresponded to alkyl ether lysoA2PE (Fig. 1; Table 1, compound 2). Thermodynamically, 1-acyl-2-lyso compounds are more stable than 1-lyso-2-acyl compounds (28). Thus, these experiments provided corroboration for the finding that an alkyl ether lysoA2PE (Fig. 4) was detected in human RPE.

Enzymatic hydrolysis of alkenyl ether lysoA2PE and A2PE by PLD and PLA₂

PLD catalyzes the cleavage of the phosphodiester bond of GPs, thereby generating phosphatidic acid and a free ethanolamine (29, 30). In the case of diacyl A2PE species, PLD-mediated cleavage produces phosphatidic acid and A2E (Fig. 1, supplemental Fig. S1). To demonstrate PLD-activity on lysoA2PE, we incubated alkenyl ether lysoA2PE(P-18:0/0:0) (Table 1, compound 6) with the enzyme. The chromatogram produced from the PLD-incubated mixture, as shown in **Fig. 5B**, revealed a peak at 7 min that was attributable to A2E (Fig. 1, supplemental Fig. S1) on the basis of UV/visible absorbance maxima (λ_{max} 337, 440 nm) and a mass value (m/z 592.5).

PLA₂ hydrolyzed the *sn*-2 fatty acyl ester bond of phosphoglycerides, producing free fatty acids and lysophospholipids (Fig. 1, supplemental Fig. S1). Because we detected lysoA2PE in human RPE, but not in neural retina (Fig. 3A, B), one possible explanation is that the A2PE species undergo hydrolysis by PLA₂ in human RPE. Therefore, to test for PLA₂ activity, plasmalogen-type A2PE {alkenyl ether acylA2PE[P-18:0/18:1(9Z)], m/z 1,261.0} (Table 1, compound 7) was employed. The structure of the latter compound contains, as in our novel alkyl ether lysoA2PE, an ether bond at the *sn*-1 site and an ester linkage at the *sn*-2 position. The latter is a target for PLA₂-mediated cleavage. After incubation with PLA₂, the hydrolyzed product, alkenyl ether lysoA2PE, having m/z 996.7 and absorbance maxima at 337 and 443 nm, appeared as a peak at 21 min in the UPLC chromatogram (**Fig. 6A,** B).

Nonenzymatic cleavage of alkenyl ether lysoAP2E under acidic conditions

We have shown previously that diacyl A2PE (A2-DPPE) synthesized by reacting diacyl GPE (DPPE) with
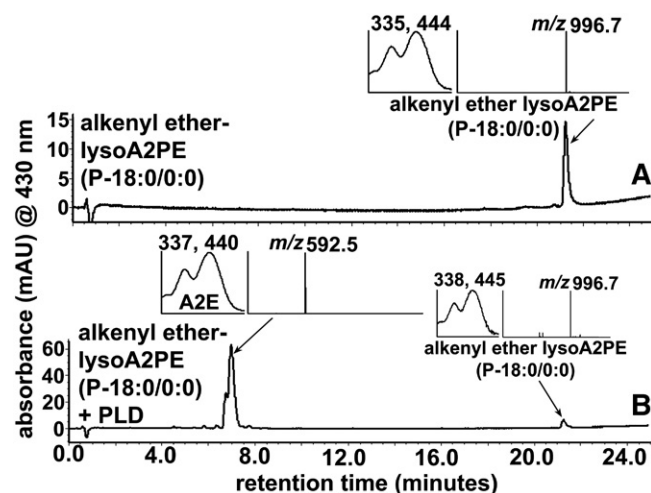
Fig. 5. Hydrolysis of alkenyl ether lysoA2PE(P-18:0/0:0) (m/z 996.7) by PLD generates A2E (m/z 592.5). A: Alkenyl ether lysoA2PE before incubation. B: Detection of alkenyl ether lysoA2PE and A2E after incubation with PLD. Starting material and cleavage products were detected by UPLC-ESI-MS and monitoring at 430 nm (UPLC condition b). Insets: UV-visible absorbance and mass spectrum of the indicated compounds. PLD cleaves at the phosphodiester bond in alkenyl ether lysoA2PE to release A2E.

Fig. 6. Hydrolysis of alkenyl ether acylA2PE[P-18:0/18:1(9Z)] (m/z 1,261.0) by PLA_2 yields alkenyl ether lysoA2PE(P-18:0/0:0) (m/z 996.7). A: A2PE before incubation. B: A2PE after incubation with PLA_2. Starting material (alkenyl ether acylA2PE) and cleavage products were detected by UPLC-ESI-MS with monitoring at 430 nm (UPLC condition b). Insets: UV-visible absorbance and mass spectra of the indicated compounds. PLA_2 cleaves at the ester bond emanating from the *sn*-2 carbon in A2PE to release alkenyl ether lysoA2PE.
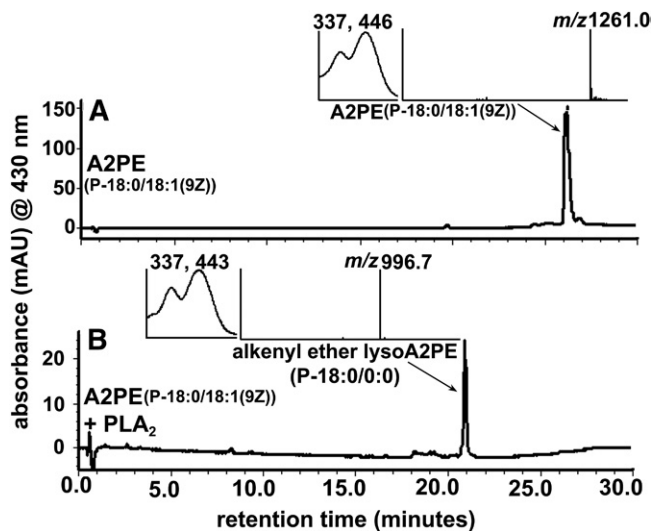

Fig. 7. Hydrolysis of alkenyl ether lysoA2PE(P-18:0/0:0) (m/z 996.7) by incubation at pH 5 in DPBS generates A2GPE (m/z 746.5). A: Alkenyl ether lysoA2PE before incubation. B:) Alkenyl ether lysoA2PE and A2GPE after incubation for 48 h at pH 5 in DPBS. Starting material (alkenyl ether lysoA2PE) and acid hydrolyzed product (A2GPE) were detected by UPLC-ESI-MS with monitoring at 430 nm (UPLC condition b). Insets: UV-visible absorbance and mass spectra of the indicated compounds.

all-*trans*-retinal, is stable at acidic conditions (pH ∼5.5 –6.0) (14). The conversion rate was only approximately 0.01% of the A2PE sample maintained at neutral pH (14). However, taking into account that among phospholipids, plasmalogens are a subclass that are major constituents of human photoreceptor outer segments, together with the acid sensitivity of the vinyl ether linkage (at *sn*-1 position) (4), one cannot exclude the possibility that plasmalogen type A2PE would be able to undergo hydrolysis by acidic environments in the RPE lysosome. Thus, we chose alkenyl ether lysoA2PE (P-18:0/0:0) (m/z 996.7) (Table 1, compound 6) as a plasmalogen-type A2PE and 2-lyso bisretinoid, which could conceivably exist in lysosomes, and tested for acid hydrolysis. As shown in **Fig. 7B**, we confirmed that hydrolytic cleavage of plasmalogen-type A2PE occurs when incubated for 2 days in phosphate buffer at pH 5. Interestingly, as a result of hydrolysis, A2GPE (Fig. 1, supplemental Fig. S1) was generated (Fig. 7B), presumably by cleavage between oxygen and the olefinic carbon of alkenyl ether lysoA2PE (31). The identification of A2GPE was corroborated by comparison to synthetic A2GPE on the basis of Rt, absorbance maxima (λ_{max} 333, 434), and mass (m/z 746.5) (Fig. 7B).

FLR emission spectra of alkenyl ether lysoA2PE

The emission spectra recorded for alkenyl ether lyso-A2PE(P-18:0/0:0) (Table 1, compound 6) in a variety of solvents resulted in either hyper/hypochromic changes and/or blue/red shifts in absorbance (**Fig. 8**). Plasmalogen (alkenyl ether) type lysoA2PE (Table 1, compound 6) rather than alkyl ether lysoA2PE (Table 1, compound 2)
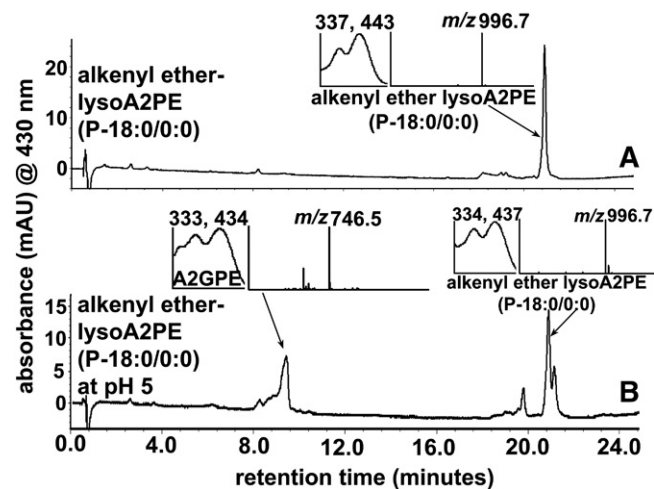
was synthesized and used for this nonenzymatic assay because of the commercial availability of the former. We have previously studied A2GPE FLR emission spectra (430 nm excitation) in various solvents including chloroform, PBS, and methanol. Among the solvents, the most intense emission was recorded in chloroform, followed by PBS and methanol (24). Here, we observed that emission spectra generated with alkenyl ether lysoA2PE in chloroform, PBS, and DMSO were similar to that of A2GPE (Fig. 8B). Relative to PBS, a hypochromic change was observed when FLR emission of alkenyl ether lysoA2PE was measured in DMSO (excitation at 440 nm), whereas a hyperchromic difference occurred when the emission spectrum was recorded in the less polar chloroform (Fig. 8B).

Because alkenyl ether lysoA2PE contains an unsaturated fatty acid long chain (supplemental Fig. S1), we also recorded emission spectra in PBS with three different types of hydrophobic environments (Fig. 8A). In trialkyl-methyl-ammonium chloride (TMAC) (1 mM in PBS, cationic), a positively charged detergent with which the cationic head group of alkenyl ether lysoA2PE would not associate, FLR emission was minimal (32). When also recorded in sodium dodecyl sulfate (SDS) (1 mM in PBS, anionic), a negatively charged surfactant, the emission intensity of alkenyl ether lysoA2PE was also lower than in PBS (with 2% DMSO) and it exhibited a hypsochromic (blue) shift relative to both TMAC and PBS. Interestingly, FLR measurement in dioleoylphosphatidylcholine (DOPC) (1 mM in PBS, neutral) revealed an appreciable hyperchromic increase (at least 3-fold higher FLR intensity than that in PBS) and a slight blue shift compared with that in PBS. The latter results were consistent with previous studies of A2E in a DOPC milieu (24, 32).
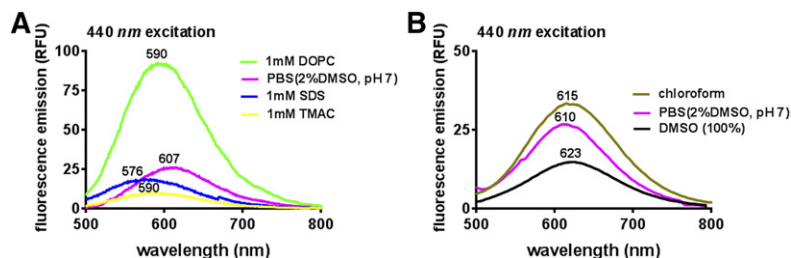
Fig. 8. FLR emission spectra of alkenyl ether lysoA2PE(P-18:0/0:0). A: Emission spectra of alkenyl ether lysoA2PE (100 μM) in DOPC (1 mM), 2% DMSO in PBS, SDS (1 mM), trialkyl-methylammonium chloride (TMAC; 1 mM), and 100% DMSO recorded from a 384-well microplate. FLR (relative FLR units, RFU) was recorded at an excitation of 440 nm. Emission maximum (nanometers) of each spectral profile is indicated. B: FLR emission spectra of alkenyl ether lysoA2PE in chloroform, 2% DMSO in PBS, and DMSO, recorded from a quartz cuvette.

Photooxidation of lysoA2PE

We compared the propensity for alkenyl ether lyso-A2PE(P-18:0/0:0) (Table 1, compound 6) and A2E to undergo photooxidation by measuring the oxidation-related consumption of these bisretinoids as a function of irradiation time (**Fig. 9**). The rate of A2E photooxidation under 430 nm exposure was greater than the photooxidative loss of alkenyl ether lysoA2PE. As a comparison, acyl lysoA2PE(18:0/0:0) (Table 1, compound 5) that bears an ester bond instead of alkenyl ether bond was also examined to explore resistance to oxidation in the presence of the vinyl ether bond. Interestingly, the photooxidation of alkenyl ether-containing lysoA2PE was slower when compared with the ester-containing lysoA2PE. These results suggest a protective role of the vinyl ether in light-induced oxidation processes. We also tested photooxidation of alkenyl ether lysoA2PE(P-18:0/0:0) when introduced to an environment of polyunsaturated fatty acid (DHA in the form of 1 mM of 1,2-didocosahexaenoyl-*sn*-glycero-3-phosphocholine), the latter being highly susceptible to light-mediated oxidation (33). Reduced photooxidative degradation of the A2-chromophore was observed in the unsaturated fatty acid milieu.

DISCUSSION

Our understanding of the burden placed on the RPE cell by the formation of phototoxic retinaldehyde-adducts (6) depends on the identification and quantitation of the various bisretinoid species that constitute this family of fluorophores. Efforts to develop therapies for various forms of macular degeneration include approaches that would target bisretinoid synthesis (34–37); these efforts can be aided by improved understanding of the biosynthetic routes.

Initial isolation and structural elucidation of A2E and isoA2E in human RPE was followed by the identification of atRALdi, atRALdi-PE, A2-DHP-PE, and A2GPE (16, 19, 24, 25, 38). These bisretinoids were characterized using spectroscopic techniques, quantitative HPLC-PDA analysis of the products of biomimetic synthesis, and quantitative analysis of these fluorophore species in photoreceptor cell outer segments and RPE (17, 18, 22, 23). All of these bisretinoids were isolated from human RPE (16, 17, 19, 24, 25). Based on our findings, we also proposed biogenesis schemes for bisretinoid formation in retina (**Fig. 10**) (13, 16, 26). We showed that, as a final step in the biosynthetic scheme, the precursor A2PE was efficiently processed by PLD-enzymatic hydrolysis to yield A2E. Accordingly, A2PE was shown not to be detectable in RPE cells (15). Until now, enzyme-mediated hydrolysis has been largely investigated using PLD (14, 15). For instance A2E was shown to be released from several bisretinoid precursors, including A2-DPPE and A2GPE, by PLD-mediated activity (18, 24). Because A2GPE does not contain fatty acid chains at either the *sn*-1 or *sn*-2 ester linkage, those previous results indicated that PLD-mediated hydrolysis at phosphodiester moieties of GP constituents of A2PE is not affected by fatty acid chains attached to the glycerol backbone. Similarly, the release of A2E from lysoA2PE (Fig. 5) reveals that PLD also cleaves the phosphodiester bond within the A2PE species regardless of the type of linkage at *sn*-1 and -2 (ester or ether).

As discussed above, the formation of NRPE from retinaldehyde and PE is the first step in the formation of A2PE and A2E. Rearrangements, reaction with a second molecule of retinaldehyde, and elimination of two hydrogens from the intermediate dihydropyridinium-A2PE yield A2PE (12, 13). Here, we have added to the biogenesis scheme by showing that PLA$_2$ can also process 1-alkyl ether-2-acyl-A2PE (i.e., an ether bond at the *sn*-1 site and an ester bond at the *sn*-2 site) by mediating cleavage at the ester bond positioned at the *sn*-2 site so as to produce lysoA2PE presenting with a single alkyl chain at the *sn*-1 position.
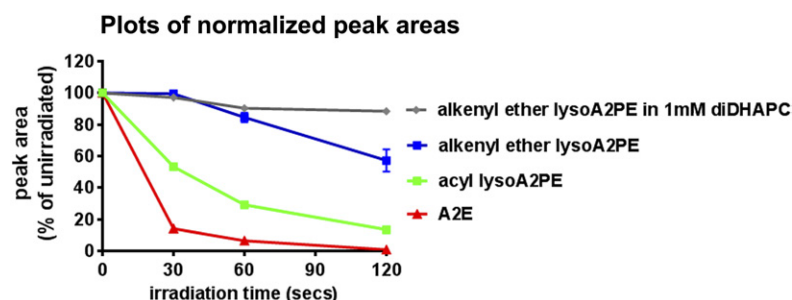

Fig. 9. Photooxidation of alkenyl ether lysoA2PE (P-18:0/0:0) (one *cis* double bond on the fatty acid chain), acyl lysoA2PE(18:0/0:0) (no double bond on the fatty acid chain), and A2E in PBS with 2% DMSO or 1 mM 1,2-didocosahexaenoyl-*sn*-glycero-3-phosphocholine in PBS with 2% DMSO. Photooxidative loss is plotted as normalized peak area and as a function of irradiation time.
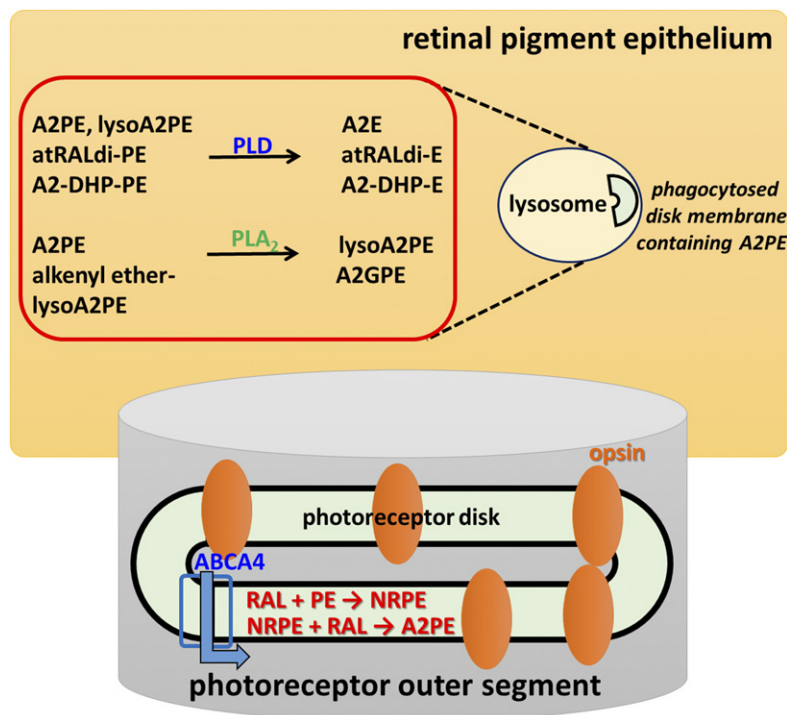
Fig. 10. Schematic summarizing bisretinoid production in photoreceptor outer segments with processing in RPE. RAL, retinaldehyde.

The unprecedented detection of the bisretinoid alkyl ether lysoA2PE, not in neural retina, but in human RPE (Fig. 3), indicates that the PLA$_2$ activity likely resides in RPE (Fig. 10). In addition, A2GPE formation by nonenzymatic hydrolysis of alkenyl type lysoA2PE in an acidic environment serves as a new mechanism contributing to the final processing of bisretinoids (Fig. 7). Notwithstanding the evidence that A2PE and lysoA2PE undergo hydrolysis by PLD, detection of GP bearing bisretinoids, such as A2GPE and lysoA2PE, suggests that other factors, such as competition among hydrolytic enzymes and/or conditions of the lysosomal micro-milieu, may modulate mechanisms responsible for hydrolysis. For instance, the latter factor may explain why some bisretinoids (e.g., A2PE) undergo facile cleavage to remove phosphatidic acid while others do not (e.g., A2-DHP-PE). On the other hand, while we did not compare PLD efficiency toward each structure, we recognize that the enzyme might have different preferences for the linkages or fatty acids either at the *sn*-1 or *sn*-2 of the structures. Figure 10 presents a biosynthetic scheme that includes enzymatic hydrolyses (Fig. 10).

It has been reported that cultured human RPE cells contain at least three different types of PLA$_2$ (iPLA$_2$-VIA, iPLA$_2$-VIB, and sPLA$_2$) (39). Moreover, several types of PLA$_2$ (iPLA$_2$-VIA, iPLA$_2$-VIB, and ciPLA$_2$-IVA) have been identified in normal human eyes by protein identification and, among them, iPLA$_2$-VIA strongly involves the regulation of RPE phagocytosis of photoreceptor outer segments (40). Interestingly, protein expression of the iPLA$_2$-VIA proteins using immunostaining of normal human eyes has revealed that staining intensity of the PLA$_2$ in RPE is much stronger than in photoreceptor outer segments (40). These reports together with the present results demonstrating that lysoA2PE is present in human RPE are consistent with the possibility that A2PE derived from phagocytosed outer segment membrane can be hydrolyzed by PLA$_2$ allowing 1-alkyl-2-lyso-*sn*-glycero A2PE to be detectable in RPE (Fig. 3A).

As with other bisretinoids, the FLR capability of lysoA2PE is provided by an extensive system of carbon-carbon double bonds within its retinaldehyde-derived chromophore. The FLR efficiency of bisretinoids is in turn influenced by the micro-environment (32) of the lysosomal organelles in which they are sequestered. The lysosomal milieu is likely heterogeneous due to the presence of polar and hydrophobic side-chains of proteins together with lipid. We previously proposed a model within which bisretinoids of RPE lipofuscin self-organize into microdomains that influence their photoreactivity and FLR efficiency (32). As we have previously reported for A2E and A2GPE, we found here that in hydrophobic solvents such as chloroform, FLR intensity was greater than in the polar milieu of PBS. Similarly, the FLR intensity of alkenyl ether lysoA2PE in hydrophobic environment of DOPC was greater than in SDS and PBS. A comparison between the emission intensity of A2E (32) versus alkenyl ether lysoA2PE in SDS suggests that, in this negatively charged surfactant (Fig. 8), A2E exhibits greater FLR emission than alkenyl-ether-lysoA2PE. The structure of alkenyl etherlysoA2PE, including the saturated hydrocarbon long chain and glycerol phosphate moieties, is more complex than A2E. Due to the negative charge on the glycerol phosphate moiety, alkenyl ether lysoA2PE is likely to resist the tight packing required to form micelles with SDS in an aqueous milieu, while A2E, with its cationic polar head group, would readily associate with SDS. On the other hand, alkenyl ether lysoA2PE may be able to aggregate in association with the hydrophobic retinaldehyde side-arms in aqueous conditions, thus conferring greater photooxidation under blue light radiation (Fig. 9).

It has been assumed that bisretinoids, and A2E in particular, accumulate in lysosomes of RPE cells because they become trapped after protonation in the acidic environment of the lysosome, thereby inhibiting lysosomal enzymes (41, 42). However A2E is a quaternary pyridinium salt that does not deprotonate or reprotonate; the positive charge on the pyridinium nitrogen is neutralized by a counterion, probably chloride (25, 26, 43). The bisretinoid A2-DHP-PE presents with an uncharged dihydropyridine ring at its core, yet this bisretinoid still accumulates in RPE lipofuscin (19). Another bisretinoid that accumulates in lysosomes is the bisretinoid, all-*trans*-retinal dimer; this fluorophore presents with a noncharged cyclohexadiene ring (16, 17). All-*trans*-retinal dimer can also form a conjugate with PE (all-*trans*-retinal dimer-PE) via a Schiff base linkage that exhibits pH-dependent protonation (17), and as with unprotonated unconjugated all-*trans*-retinal dimer, all-*trans*-retinal dimer-PE accumulates in RPE lysosomes (17). Moreover, as we have shown here, the final step in the formation of A2E, A2GPE, and lysoA2PE, all of which are amassed in RPE lysosomes, depends on the activity of at least two hydrolytic enzymes, PLD and PLA$_2$. Taken together, these findings indicate that inhibition of lysosomal activity is unlikely to be the reason why bisretinoids accumulate. Reduced activity of lysosomal degradative enzymes, if it were to occur, would result in a generalized increase in protein/peptide accumulation as in lysosomal storage diseases (44), but this is not observed (45). Moreover, it is worth noting that all healthy eyes accumulate bisretinoid beginning early in life.

To date, several bisretinoids of RPE lipofuscin have been isolated and characterized, and for all of these formation involves the membrane phospholipid, PE. The bisretinoid composition of RPE lipofuscin has been analyzed in human, rat, mouse, and bovine eyes and, in all cases, the same pigments are observed, although the relative levels of one bisretinoid to another can vary. In future experiments, we will analyze and measure alkyl ether lysoA2PE in mutant mouse models to determine how the prevalence of this fluorophore species varies with age and retinal disease.⬛

REFERENCES

1. Fahy, E., S. Subramaniam, H. A. Brown, C. K. Glass, A. H. Merrill, Jr., R. C. Murphy, C. R. Raetz, D. W. Russell, Y. Seyama, W. Shaw, et al. 2005. A comprehensive classification system for lipids. *J. Lipid Res.* **46:** 839–861.
2. Braverman, N. E., and A. B. Moser. 2012. Functions of plasmalogen lipids in health and disease. *Biochim. Biophys. Acta.* **1822:** 1442–1452.
3. Vandeenen, L. L., and G. H. Dehaas. 1966. Phosphoglycerides and phospholipases. *Annu. Rev. Biochem.* **35:** 157–194.
4. Nagan, N., and R. A. Zoeller. 2001. Plasmalogens: biosynthesis and functions. *Prog. Lipid Res.* **40:** 199–229.
5. Fliesler, S. J., and R. E. Anderson. 1983. Chemistry and metabolism of lipids in the vertebrate retina. *Prog. Lipid Res.* **22:** 79–131.
6. Ueda, K., J. Zhao, H. J. Kim, and J. R. Sparrow. 2016. Photodegradation of retinal bisretinoids in mouse models and implications for macular degeneration. *Proc. Natl. Acad. Sci. USA.* **113:** 6904–6909.
7. Anderson, R. E., and M. B. Maude. 1970. Phospholipids of bovine outer segments. *Biochemistry.* **9:** 3624–3628.
8. Illing, M., L. L. Molday, and R. S. Molday. 1997. The 220-kDa rim protein of retinal rod outer segments is a member of the ABC transporter superfamily. *J. Biol. Chem.* **272:** 10303–10310.
9. Papermaster, D. S., B. G. Schneider, M. A. Zorn, and J. P. Kraehenbuhl. 1978. Immunocytochemical localization of opsin in outer segments and Golgi zones of frog photoreceptor cells. An electron microscope analysis of cross-linked albumin-embedded retinas. *J. Cell Biol.* **77:** 196–210.
10. Sun, H., R. S. Molday, and J. Nathans. 1999. Retinal stimulates ATP hydrolysis by purified and reconstituted ABCR, the photoreceptor-specific ATP-binding cassette transporter responsible for Stargardt disease. *J. Biol. Chem.* **274:** 8269–8281.
11. Sun, H., and J. Nathans. 1997. Stargardt's ABCR is localized to the disc membrane of retinal rod outer segments. *Nat. Genet.* **17:** 15–16.
12. Kim, S. R., J. He, E. Yanase, Y. P. Jang, N. Berova, J. R. Sparrow, and K. Nakanishi. 2007. Characterization of dihydro-A2PE: an intermediate in the A2E biosynthetic pathway. *Biochemistry.* **46:** 10122–10129.
13. Sparrow, J. R., E. Gregory-Roberts, K. Yamamoto, A. Blonska, S. K. Ghosh, K. Ueda, and J. Zhou. 2012. The bisretinoids of retinal pigment epithelium. *Prog. Retin. Eye Res.* **31:** 121–135.
14. Ben-Shabat, S., C. A. Parish, H. R. Vollmer, Y. Itagaki, N. Fishkin, K. Nakanishi, and J. R. Sparrow. 2002. Biosynthetic studies of A2E, a major fluorophore of retinal pigment epithelial lipofuscin. *J. Biol. Chem.* **277:** 7183–7190.
15. Sparrow, J. R., S. R. Kim, A. M. Cuervo, and U. Bandhyopadhyayand. 2008. A2E, a pigment of RPE lipofuscin, is generated from the precursor, A2PE by a lysosomal enzyme activity. *Adv. Exp. Med. Biol.* **613:** 393–398.
16. Fishkin, N. E., J. R. Sparrow, R. Allikmets, and K. Nakanishi. 2005. Isolation and characterization of a retinal pigment epithelial cell fluorophore: an all-trans-retinal dimer conjugate. *Proc. Natl. Acad. Sci. USA.* **102:** 7091–7096.
17. Kim, S. R., Y. P. Jang, S. Jockusch, N. E. Fishkin, N. J. Turro, and J. R. Sparrow. 2007. The all-trans-retinal dimer series of lipofuscin pigments in retinal pigment epithelial cells in a recessive Stargardt disease model. *Proc. Natl. Acad. Sci. USA.* **104:** 19273–19278.
18. Liu, J., Y. Itagaki, S. Ben-Shabat, K. Nakanishi, and J. R. Sparrow. 2000. The biosynthesis of A2E, a fluorophore of aging retina, involves the formation of the precursor, A2-PE, in the photoreceptor outer segment membrane. *J. Biol. Chem.* **275:** 29354–29360.
19. Wu, Y., N. E. Fishkin, A. Pande, J. Pande, and J. R. Sparrow. 2009. Novel lipofuscin bisretinoids prominent in human retina and in a model of recessive Stargardt disease. *J. Biol. Chem.* **284:** 20155–20166.
20. Bok, D. 1993. The retinal pigment epithelium: a versatile partner in vision. *J. Cell Sci. Suppl.* **17:** 189–195.
21. Kim, S. R., N. Fishkin, J. Kong, K. Nakanishi, R. Allikmets, and J. R. Sparrow. 2004. Rpe65 Leu450Met variant is associated with reduced levels of the retinal pigment epithelium lipofuscin fluorophores A2E and iso-A2E. *Proc. Natl. Acad. Sci. USA.* **101:** 11668–11672.
22. Mata, N. L., J. Weng, and G. H. Travis. 2000. Biosynthesis of a major lipofuscin fluorophore in mice and humans with ABCR-mediated retinal and macular degeneration. *Proc. Natl. Acad. Sci. USA.* **97:** 7154–7159.
23. Weng, J., N. L. Mata, S. M. Azarian, R. T. Tzekov, D. G. Birch, and G. H. Travis. 1999. Insights into the function of Rim protein in photoreceptors and etiology of Stargardt's disease from the phenotype in abcr knockout mice. *Cell.* **98:** 13–23.
24. Yamamoto, K., K. D. Yoon, K. Ueda, M. Hashimoto, and J. R. Sparrow. 2011. A novel bisretinoid of retina is an adduct on glycerophosphoethanolamine. *Invest. Ophthalmol. Vis. Sci.* **52:** 9084–9090.
25. Parish, C. A., M. Hashimoto, K. Nakanishi, J. Dillon, and J. Sparrow. 1998. Isolation and one-step preparation of A2E and iso-A2E, fluorophores from human retinal pigment epithelium. *Proc. Natl. Acad. Sci. USA.* **95:** 14609–14613.
26. Sparrow, J. R., Y. L. Wu, C. Y. Kim, and J. L. Zhou. 2010. Phospholipid meets all-trans-retinal: the making of RPE bisretinoids. *J. Lipid Res.* **51:** 247–261.
27. Martinez, M., A. Ballabriga, and J. J. Gil-Gibernau. 1988. Lipids of the developing human retina: I. Total fatty acids, plasmalogens, and fatty acid composition of ethanolamine and choline phosphoglycerides. *J. Neurosci. Res.* **20:** 484–490.
28. Pencreac'h, G., F. Ergan, and L. Poisson. 2013. DHA-lysophospholipid production. *Curr. Org. Chem.* **17:** 793–801.
29. McDermott, M., M. J. Wakelam, and A. J. Morris. 2004. Phospholipase D. *Biochem. Cell Biol.* **82:** 225–253.

30. Giusto, N. M., S. J. Pasquare, G. A. Salvador, and M. G. Ilincheta de Boschero. 2010. Lipid second messengers and related enzymes in vertebrate rod outer segments. *J. Lipid Res.* **51:** 685–700.

31. Fife, T. H. 1965. Vinyl ether hydrolysis - facile general acid catalyzed conversion of 2-ethoxy-1-cyclopentene-1-carboxylic acid to cyclopentanone. *J. Am. Chem. Soc.* **87:** 1084–1089.

32. Liu, Z., K. Ueda, H. J. Kim, and J. R. Sparrow. 2015. Photobleaching and fluorescence recovery of RPE bisretinoids. *PLoS One.* **10:** e0138081.

33. Tanito, M., R. S. Brush, M. H. Elliott, L. D. Wicker, K. R. Henry, and R. E. Anderson. 2009. High levels of retinal membrane docosahexaenoic acid increase susceptibility to stress-induced degeneration. *J. Lipid Res.* **50:** 807–819.

34. Sparrow, J. R. 2016. Vitamin A-aldehyde adducts: AMD risk and targeted therapeutics. *Proc. Natl. Acad. Sci. USA.* **113:** 4564–4569.

35. Mata, N. L., J. B. Lichter, R. Vogel, Y. Han, T. V. Bui, and L. J. Singerman. 2013. Investigation of oral fenretinide for treatment of geographic atrophy in age-related macular degeneration. *Retina.* **33:** 498–507.

36. Dobri, N., Q. Qin, J. Kong, K. Yamamoto, Z. Liu, G. Moiseyev, J. X. Ma, R. Allikmets, J. R. Sparrow, and K. Petrukhin. 2013. A1120, a nonretinoid RBP4 antagonist, inhibits formation of cytotoxic bisretinoids in the animal model of enhanced retinal lipofuscinogenesis. *Invest. Ophthalmol. Vis. Sci.* **54:** 85–95.

37. Mata, N. L., and R. Vogel. 2010. Pharmacologic treatment of atrophic age-related macular degeneration. *Curr. Opin. Ophthalmol.* **21:** 190–196.

38. Sakai, N., J. Decatur, K. Nakanishi, and G. E. Eldred. 1996. Ocular age pigment "A2-E": An unprecedented pyridinium bisretinoid. *J. Am. Chem. Soc.* **118:** 1559–1560.

39. Van Themsche, C., M. Jacob, and C. Salesse. 2001. Human retinal pigment epithelium secretes a phospholipase A2 and contains two novel intracellular phospholipases A2. *Biochem. Cell Biol.* **79:** 1–10.

40. Kolko, M., J. Wang, C. Zhan, K. A. Poulsen, J. U. Prause, M. H. Nissen, S. Heegaard, and N. G. Bazan. 2007. Identification of intracellular phospholipases A2 in the human eye: involvement in phagocytosis of photoreceptor outer segments. *Invest. Ophthalmol. Vis. Sci.* **48:** 1401–1409.

41. Eldred, G. E., and M. R. Lasky. 1993. Retinal age pigments generated by self-assembling lysosomotropic detergents. *Nature.* **361:** 724–726.

42. Liu, J., W. Lu, D. Reigada, J. Nguyen, A. M. Laties, and C. H. Mitchell. 2008. Restoration of lysosomal pH in RPE cells from cultured human and ABCA4(−/−) mice: pharmacologic approaches and functional recovery. *Invest. Ophthalmol. Vis. Sci.* **49:** 772–780.

43. Sparrow, J. R., C. A. Parish, M. Hashimoto, and K. Nakanishi. 1999. A2E, a lipofuscin fluorophore, in human retinal pigmented epithelial cells in culture. *Invest. Ophthalmol. Vis. Sci.* **40:** 2988–2995.

44. Brady, R. O. 2006. Emerging strategies for the treatment of hereditary metabolic storage disorders. *Rejuvenation Res.* **9:** 237–244.

45. Ng, K. P., B. Gugiu, K. Renganathan, M. W. Davies, X. Gu, J. S. Crabb, S. R. Kim, M. B. Rozanowska, V. L. Bonilha, M. E. Rayborn, et al. 2008. Retinal pigment epithelium lipofuscin proteomics. *Mol. Cell. Proteomics.* **7:** 1397–1405.